Journal of Mines, Metals and Fuels, *73(5): 1343-1354; 2025. DOI: 10.18311/jmmf/2025/48664*

Print ISSN : 0022-2755

Journal of Mines, Metals and Fuels

Contents available at: *www.informaticsjournals.co.in/index.php/jmmf*

Finite Element Analysis and Design Optimization of a Paddle Mixer Shaft

Sukhadip Mhankali Chougule[1,2], Govindarajan Murali[1]* and Anant Sidhappa Kurhade[3,4]

[1]Department of Mechanical Engineering, Koneru Lakshmaiah Education Foundation, Green Fields, Vaddeswaram, Guntur (Dt) - 522502, Andhra Pradesh, India; muralinitt@gmail.com

[2]Department of Mechanical Engineering, PCET's Pimpri Chinchwad College of Engineering and Research, Ravet, Pune - 412101, Maharashtra, India

[3]Department of Mechanical Engineering, Dr. D. Y. Patil Institute of Technology, Sant Tukaram Nagar, Pimpri, Pune - 411018, Maharashtra, India

[4]School of Technology and Research, Dr. D. Y. Patil Dnyan Prasad University, Sant Tukaram Nagar, Pimpri, Pune - 411018, Maharashtra, India

Abstract

Mixing operations play a vital role in various industrial processes, with the structural integrity of mixer shafts being crucial for optimal performance and reliability. This study investigates the design, modeling, and Finite Element Analysis (FEA) of a paddle mixer shaft, comparing two configurations—one with stiffeners and one without. The shaft assembly, including components such as the pipe, end shafts, stiffeners, and paddles, was modeled using Pro-E software, while ANSYS 13.0 was used for FEA to assess stress distribution, deformation, and structural performance under applied loading conditions. A static analysis was conducted, considering self-weight, gravity, and applied pressure of 0.77 MPa, with uniform boundary conditions applied to both configurations. The results indicate that the stiffened paddle shaft exhibited lower maximum stress (105.26 MPa) and deformation (1.5 mm) compared to the shaft without stiffeners (173.05 MPa stress and 2.1 mm deformation). Theoretical calculations confirmed that stress values remained within permissible limits for Stainless Steel (SS), making the stiffened shaft the preferred design. Additionally, the study explores potential weight reduction by replacing SS with carbon/epoxy composite materials, demonstrating significant weight savings while maintaining structural integrity. Manufacturing processes, material specifications, and experimental validation through hydrostatic and load trials confirmed the reliability of the selected design. The trials showed an 8% deviation between experimental and simulated deformation, reinforcing the accuracy of the FEA approach. This research underscores the importance of structural reinforcement in paddle mixer shafts and provides valuable insights into design optimization, material selection, and performance validation. Future studies could explore further weight reduction using advanced composites, ensuring both durability and cost-effectiveness.

Major Findings: *The study revealed that the stiffened paddle shaft exhibited superior structural performance, with lower maximum stress (105.26 MPa) and deformation (1.5 mm) compared to the unstiffened shaft (173.05 MPa stress and 2.1 mm deformation), highlighting the effectiveness of stiffeners in enhancing structural integrity. Experimental validation through a hydrostatic test at 7.7×10^{-2} MPa showed an 8% deviation between Finite Element Analysis (FEA) predictions and experimental results, confirming the accuracy of the simulation approach. Additionally, the study explored the potential of replacing stainless steel with carbon/epoxy composites, demonstrating significant weight reduction while maintaining mechanical strength and durability, offering insights into future lightweight design optimizations.*

Keywords: *ANSYS, Composite Materials, Design Optimization, Experimental Validation, Finite Element Analysis, Manufacturing, Paddle Mixer Shaft, Structural Reinforcement*

**Author for correspondence*

1.0 Introduction

Paddle mixers are extensively used across industries such as food processing, pharmaceuticals, chemicals, and construction for blending and mixing various materials. Their efficiency depends on achieving a homogeneous mixture within an optimal timeframe, which is largely influenced by the design and performance of the mixing shaft and paddles. An inadequately designed shaft can result in inefficient mixing, higher power consumption, and premature failure due to excessive stresses. Thus, optimizing paddle mixer shaft design is essential for improving mixing efficiency, reducing operational costs, and ensuring structural integrity. FEA plays a key role in this optimization by providing an accurate assessment of mechanical performance under different operating conditions. This method enables the consideration of critical factors such as bearing elasticity and shaft deflection, which are vital for enhancing the mixer's efficiency and durability.

Bearing elasticity and clearance significantly impact shaft deflection and vibration, often neglected in existing literature or simplified using linear models despite their nonlinear behavior. This study investigates the influence of bearing nonlinearity and sealing devices (acting as a third bearing) on shaft stiffness, proposing a novel calculation method validated against FEM for determining the elastic line of a vertical cantilever shaft[1]. For Kneading Mixer paddle optimization, five independent parameters (material pot diameter, minimum clearance, hollow paddle helix angle, and two paddle angular velocities) were selected to define the paddle geometry. Geometric relationships and constraints were established, enabling the parametric design of complex paddles using Pro/E[2,3]. The study explores the application of semi-analytical finite elements in machine design, focusing on mechanical shafts under combined axial, torsional, bending, and shear loads. By utilizing Fourier series expansion and semi-analytical plane finite elements, the method offers significant computational advantages over traditional 3D FEA while maintaining accuracy in stress and displacement calculations[4]. Biodiesel production via transesterification requires intense mixing of immiscible oil and alcohol phases to enhance reaction rates and yields. This study focuses on agitator design parameters in biodiesel reactors, including power requirements, stress analysis (analytical and FEM), and operational limitations like shaft deflection and critical speed, addressing a gap in existing literature[5]. The study optimizes a passive static mixer for injection molding of non-Newtonian polymers using Taguchi methodology, focusing on four geometric parameters. Moldex3D, ANSYS Fluent, and Image J simulations validate the optimized design, demonstrating improved temperature uniformity and a higher mixing index compared to the original configuration[6]. High-capacity, high-speed washing machines subject their drum support shafts to complex bending and twisting stresses, impacting fracture strength and fatigue life. This study uses a DOE-based FEM approach with the Box-Behnken method to optimize the serrated connection between the shaft and flange, considering various design factors under combined loading and vibration[7]. Flow interferences in dual-impeller stirred tanks reduce mixing efficiency. This study uses Euler-Euler simulations and PIV experiments to analyze flow characteristics and optimize stirrer geometry via the Sobol method. The optimized design demonstrates improved solid-liquid suspension, reduced power consumption (15.6%), and increased cloud height (8.7%), validated by PIV tests[8]. Mixing system design parameters significantly influences product quality, but their effects are understudied. This DEM study investigates the impact of paddle angle, width, and gap on twin paddle blender performance, revealing optimal mixing at 0° paddle angle (though with higher particle forces), paddle width as a critical factor, and minimal influence from paddle gap on mixing efficiency and power consumption (which is minimized at 60° angle)[9]. A modified paddle mixer was designed for improved homogenization of viscoplastic materials like concrete, crucial for achieving desired mechanical properties. Dimensionless characteristics and the Metzner-Otto constant were determined, enabling the mixer's use as an onsite rheometer for rapid rheological evaluation[10]. Smartphones operating within the 2-6W power range often encounter thermal challenges due to high-performance applications, including gaming and camera processing[11]. This study investigates the application of passive Phase Change Material (PCM) cooling to maintain component temperatures below 85°C, presenting an alternative to conventional cooling techniques such as heat pipes and convection, which struggle under high-power conditions[12]. The research incorporates simulations using FR4, silicon, and

copper-clad boards with nine components, tested under different airflow conditions[13]. Results indicate that copper cladding significantly improves cooling efficiency, lowering component temperatures to 30-47 °C at 5 m/s airflow, reducing the required airflow rate by 2 m/s, and enhancing IC chip thermal management by 1.50-11.12 °C compared to the other materials[14]. Additionally, a novel minichannel PCM cooling system was analyzed, demonstrating the superior performance of N-Eicosane, which reduced temperature from 53.234°C to 51.520°C, surpassing paraffin wax and ATP 78 by 0.5°C and 1.35°C, respectively[15]. Further advancements in cooling technologies involve minijet impingement cooling[16], nanofluids[17], water-efficient faucet designs[18], and twisted tape heat transfer enhancements[19-21]. A comprehensive review of electronic cooling methods discusses their efficacy in extreme conditions, while studies on *Calophyllum inophyllum* biodiesel with dimethyl carbonate optimize engine emissions and performance[22]. Research on solar collectors utilizing recycled aluminum cans enhances drying efficiency, and numerical investigations explore substrate board thermal conductivity for improved electronic cooling. Additionally, aerodynamic studies leverage CFD and wind tunnel analysis, while fuzzy logic-based heat transfer predictions highlight the benefits of twisted tape inserts in heat exchangers[23-31]. Studies on wavy corrugated twisted tape inserts demonstrate significant heat transfer improvements, with performance evaluations emphasizing their effectiveness in forced convection. Further electronic cooling research examines thermal performance across various substrate materials, integrating PCM for smartphone circuit cooling. The wind rose analysis is used to evaluate temperature variations in wind turbines, and investigations on overlapping angles in arc-welded curved plates analyze their impact on strength and deformation[32-36]. A comparative study assesses the performance of mono-composite and metal leaf springs, while real-time surface finish measurement of stepped holding shafts is automated for precision. CFD simulations of counter-flow helical double-pipe heat exchangers, algorithmic HVACR duct design, and nanofluid applications further enhance thermal management in heat exchangers. Additionally, novel energy-absorbing bumper designs are explored for vehicle safety, while green adsorbents such as *Tinospora cordifolia* biocarbon are examined for heavy metal removal, particularly zinc ions[37-40]. Research into Transformation-Induced Plasticity (TRIP) steel plate thickness reveals its influence on the ultimate tensile strength of Nd:YAG laser butt-welded joints, impacting weld integrity. Meanwhile, experimental studies on mild steel curved plates assess their mechanical behavior under varying thicknesses. Computational research explores IC chip thermal management using PCM, while fuzzy logic modeling predicts heat transfer efficiency in double-pipe heat exchangers with wavy twisted tape inserts. Lastly, an analysis of oxygen-containing additives in unleaded gasoline examines their effects on exhaust emissions, highlighting potential environmental benefits[41-48].

This research primarily aims to analyze the structural integrity and mechanical performance of a paddle mixer shaft using FEA. The study compares two shaft configurations: Case 1 (with stiffeners) and Case 2 (without stiffeners). To achieve this, a static structural analysis is performed in ANSYS 13.0 to evaluate the maximum stress distribution under real-world operating conditions. Additionally, the study investigates the deformation characteristics under applied loads and examines how the inclusion of stiffeners improves structural performance. Beyond structural analysis, the research also explores the feasibility of replacing Stainless Steel (SS) with composite materials, specifically carbon/epoxy, to achieve weight reduction while maintaining mechanical strength and durability.

2.0 Modelling

The paddle mixer shaft was designed using Pro-E software, a feature-based solid modelling system widely used for mechanical design automation. This software enables precise geometric representation and assembly of mechanical components, facilitating detailed structural analysis.

2.1 Components of the Paddle Mixer Shaft

The paddle mixer shaft consists of several key components; each modelled separately and then assembled to form the complete structure. Figure 1 shows all the components of the paddle mixer shaft.

2.1.1 Pipe

The paddle mixer shaft, the primary structural component for paddle attachment, is made of stainless steel (density 7850 N/m^3) and measures 2044 mm in length, with an outer diameter of 90 mm and an inner diameter of 80 mm.

2.1.2 End Shafts

Two solid bars connect to the main pipe, providing support and rotational motion. They are manufactured from 90 mm diameter stainless steel bars, with lengths varying based on design requirements. Bearings support the end shafts for integration with the main drive system.

2.1.3 Stiffeners

Stiffeners enhance the strength and stability of the paddles. They are 12 mm thick, 25 mm wide and 153 mm long. Thirty-eight stiffeners, made of SA 240 TP 304 stainless steel, are assembled in pairs and welded to the main pipe and paddle bar.

2.1.4 Paddle Plate

The paddle plates are the mixing elements responsible for agitation. Each plate is 8 mm thick, 130 mm wide, and 160 mm long. Nineteen paddle plates are used, each attached to a 30 mm diameter, 178 mm long supporting bar. The supporting bars and plates are welded to the main pipe at a 45-degree angle to the shaft axis.

2.2 Assembly Process

After individually modelling the components, they were assembled to create the complete paddle mixer shaft. The final assembly includes:

- Paddle plates with supporting bars welded to the main pipe.

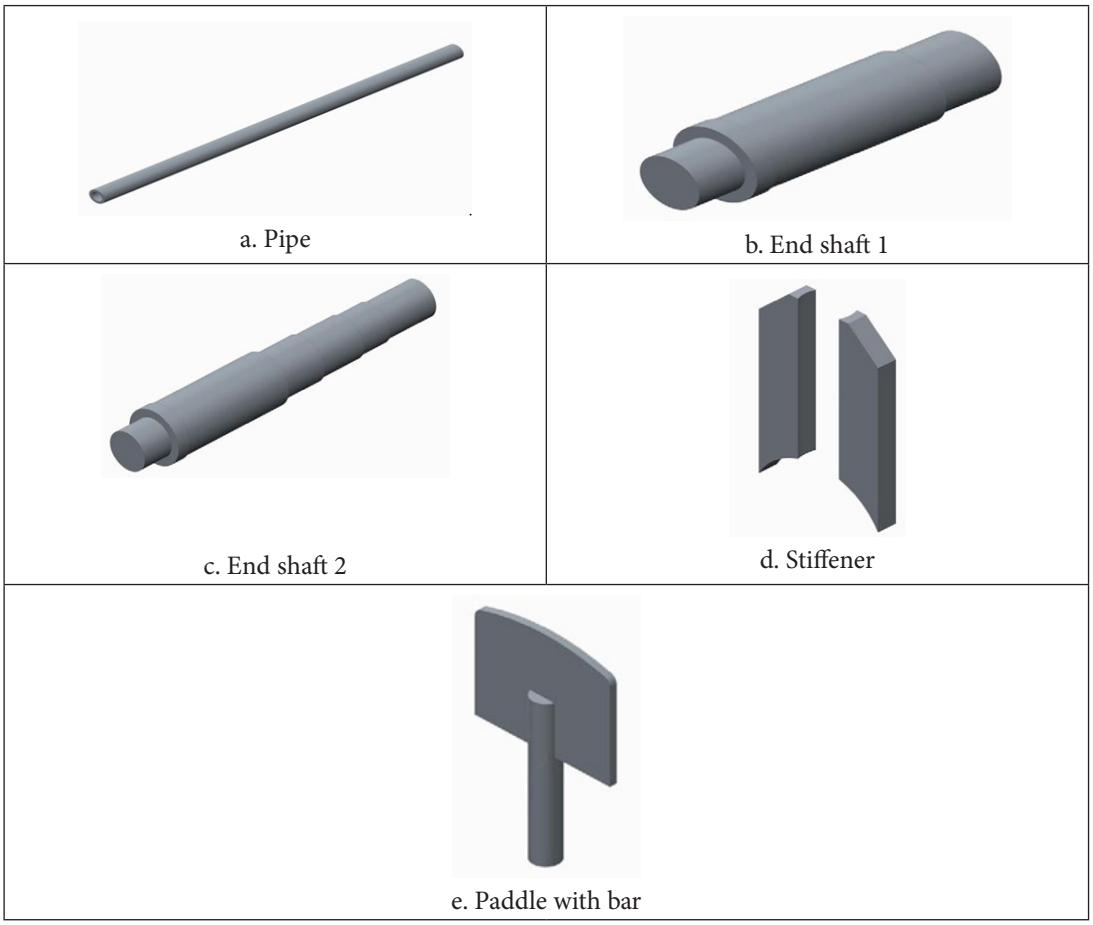


Figure 1. Components of the paddle mixer shaft.



Figure 2. Assembly.

- Stiffeners attached to the pipe and paddle bar assembly.
- End shafts integrated into the main pipe to facilitate rotational movement.

The fully assembled shaft model was then exported for FEA in ANSYS 13.0, where boundary conditions, material properties, and external forces were applied to evaluate structural performance as shown in Figure 2.

3.0 Analysis

FEA was conducted to evaluate the structural performance of the paddle mixer shaft under different loading conditions. The analysis aimed to determine the stress distribution, deformation characteristics, and the effectiveness of stiffeners in enhancing structural integrity. The simulations were performed using ANSYS 13.0, a widely used FEA software for structural analysis.

3.1 Static Structural Analysis

A static analysis was carried out to assess the **displacement, stresses, forces, and strains** in the paddle mixer shaft. The analysis included **steady inertia loads**, such as **gravity and applied pressure**. The objective was to ensure that the structure could withstand operational loads **without exceeding permissible stress limits**, which could otherwise lead to failure.

The study considered two design cases:

Case 1: Paddle shaft with stiffeners.

Case 2: Paddle shaft without stiffeners.

The same **boundary conditions and pressure loads (7.7×10^{-2} MPa)** were applied to both cases to ensure a **fair comparison**.

3.1.1 Case 1: Paddle shaft with stiffeners

Figure 3 illustrates the assembled paddle shaft, which is utilized in a mixer for blending applications. The

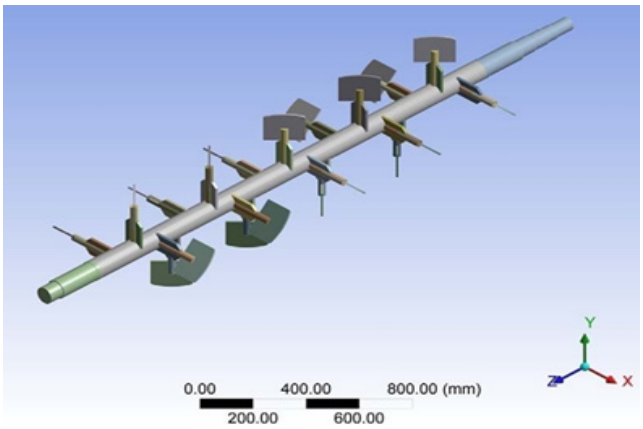


Figure 3. Paddle shaft model case 1.

model was developed using PRO/E software, where individual components of the paddle shaft were designed and subsequently assembled. The final assembly was then exported for analysis to evaluate its structural performance.

3.1.2 Boundary Conditions

Two primary boundary conditions were applied to the paddle mixer shaft as shown in Figure 4.

1. Self-weight and gravity acting downward.
2. Gravity acting downward combined with the applied design pressure (7.7×10^{-2} MPa).

The results from this analysis were used to identify areas of high-stress concentration and determine whether stiffeners provided structural reinforcement to the shaft.

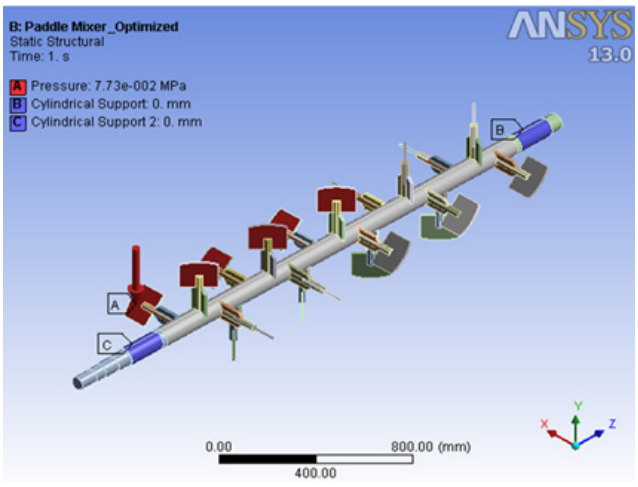


Figure 4. Boundary conditions.

3.1.3 Meshing

Tetrahedron and hex-dominant elements were utilized to determine the maximum deflections and stresses in the paddle shaft. The analysis was performed with an automatically generated mesh, adjusting the number of nodes and element size accordingly. The highest number of nodes used in the analysis was 109,189, allowing for an accurate assessment of the maximum deformation and stress distribution on the paddle shaft.

Figure 5 depicts the meshing of the paddle shaft, utilizing tetrahedron and hex-dominant elements, ensuring an optimal mesh with approximately 100,000 nodes. Figure 6 presents a graph illustrating the relationship between the number of elements and element metrics for second-order tetrahedron and hex elements.

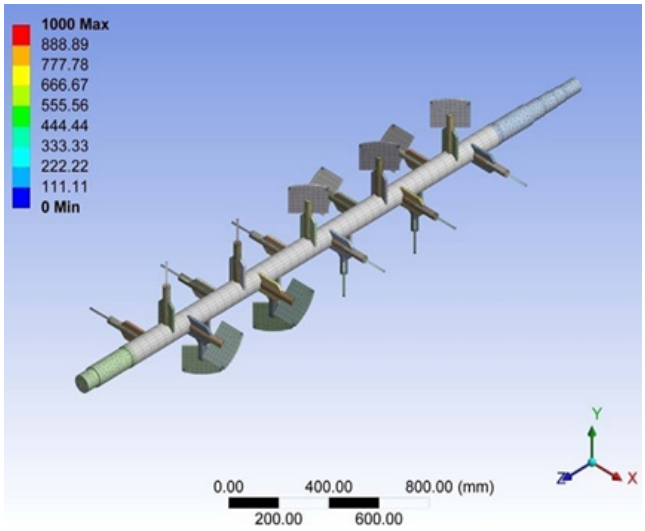


Figure 5. Case 1 meshing.

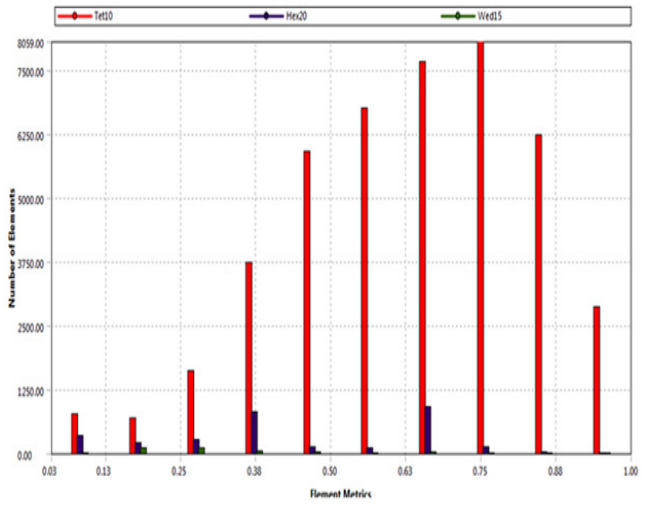


Figure 6. Element metrics vs. node count for case 1.

3.1.4. Solutions

Figure 7 presents the stress distribution on the paddle mixer shaft, with the highest stress recorded at 105.26 MPa (red) and the lowest stress near zero (blue). The peak stress concentration occurs in the midsection, indicating potential failure zones. Figure 8 illustrates the total deformation of the loaded shaft, revealing a maximum displacement of 1.5452 mm at the midsection, aligning with the region of highest stress. Minimal to no

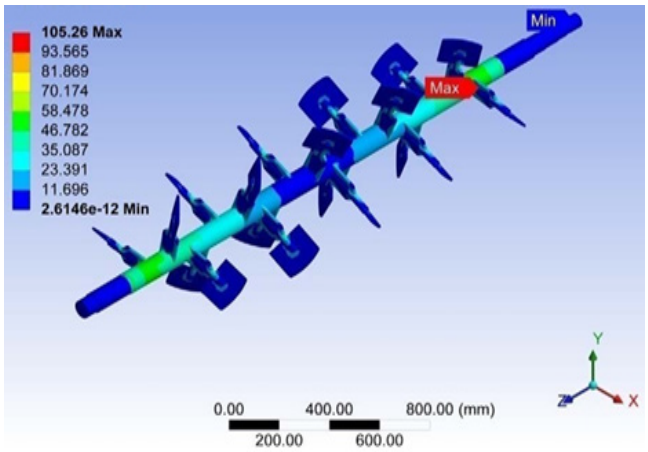


Figure 7. Maximum stresses in paddle shaft case1.

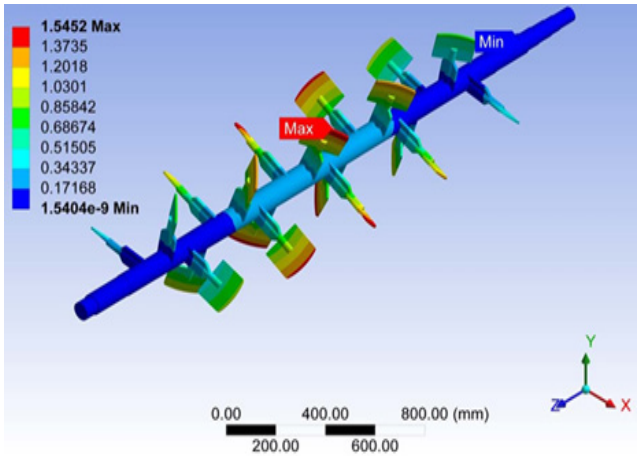


Figure 8. Maximum deformation for case 1.

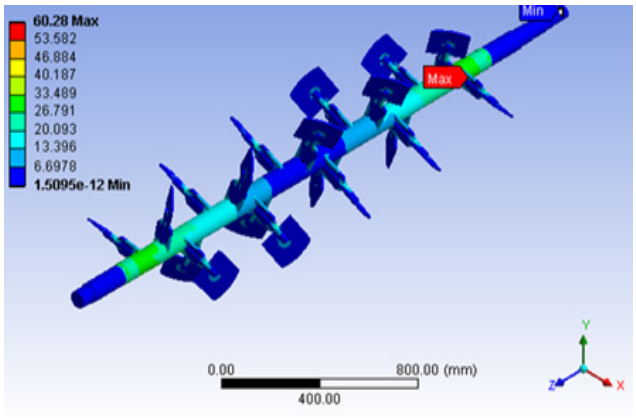


Figure 9. Maximum shear stress for case 1

displacement is observed at the shaft's fixed or supported ends. The color gradient highlights increased displacement along the paddle edges due to applied mechanical forces. Figure 9 showcases the shear stress distribution within the shaft, with a peak value of 60.28 MPa occurring in the same region as the maximum Von Mises stress. Near-zero shear stress values are represented in blue. The shear stress distribution closely follows the Von Mises stress pattern, indicating a significant contribution of shear forces to the overall structural stress.

3.2 Case 2: Paddle Shaft without Stiffeners

The accompanying figure 10 illustrates Case 1, a paddle shaft without stiffeners. The paddle plate and its supporting bar are directly attached to the main pipe, as shown. All dimensions are consistent with those described in the model section; the sole difference between this case and others is the absence of stiffeners supporting the paddle bar. This paddle plate and bar assembly is inserted into the main pipe.

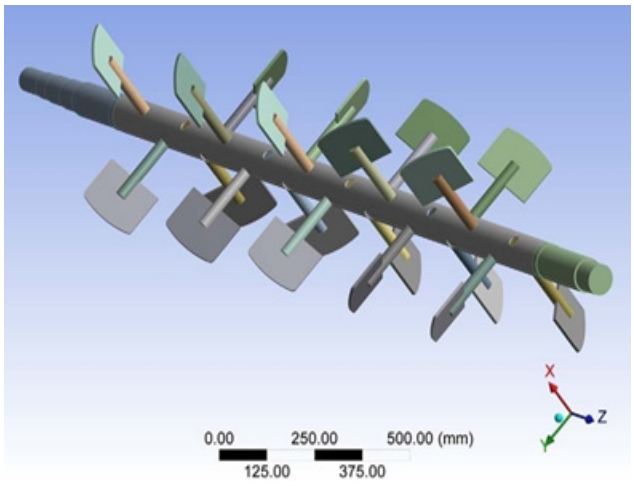


Figure 10. Paddle shaft case 2.

3.2.1 Boundary Conditions

The paddle shaft was analysed under two loading conditions: 1) its own weight and gravity, and 2) gravity combined with an internal design pressure of 7.7×10^-2 MPa. In both cases, appropriate boundary conditions were applied to the shaft as shown in Figure 11.

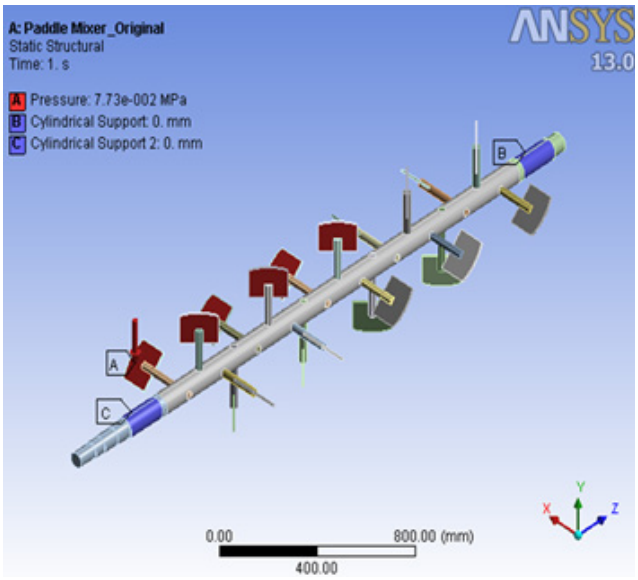


Figure 11. Boundary conditions for case 2.

3.2.2 Meshing

The maximum deflection and stress values were evaluated using tetrahedral and hexahedral-dominant elements. The analysis utilized automatically generated meshes, reaching a maximum node count of 178,514, ensuring precise computation of deformation and stress in the paddle shaft. Meshing, which involves dividing the solid model into smaller elements connected by nodes, plays a critical role in FEA for achieving accurate results.

Maximum deflection and stress values were determined using tetrahedral and hexahedral-dominant elements. The analyses employed automatically generated meshes, with a maximum node count of 178,514. This nodal density allowed for accurate calculation of maximum deformation and stress in the paddle

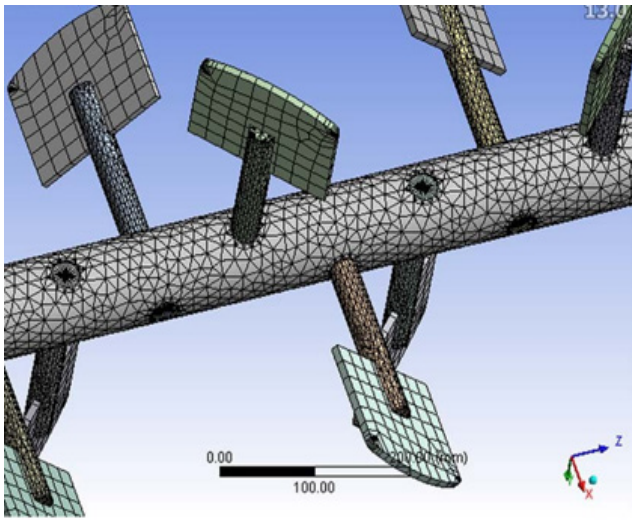


Figure 12. Case 2 meshing.

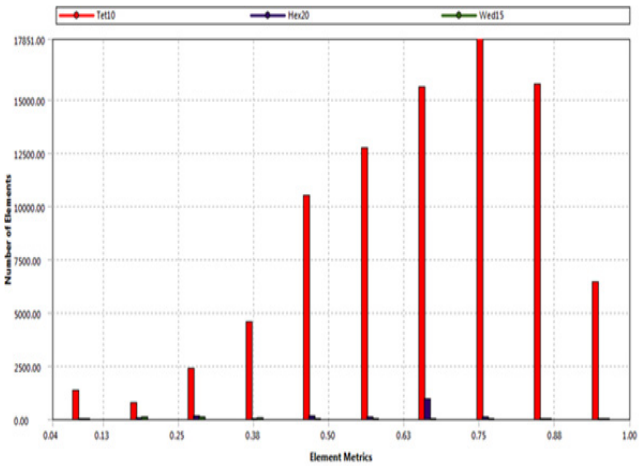


Figure 13. Element metrics vs number of nodes for case 2.

shaft. Meshing, the process of discretizing the solid model into elements composed of nodes, is crucial for finite element analysis explained in Figure 12 and Figure 13.

3.2.3 Solutions

Figure 14 illustrates the Von Mises stress distribution on the original paddle mixer shaft. The maximum stress of 173.09 MPa (red) represents the highest stress concentration point, while the minimum stress is close to zero (7.84e-12 MPa, blue). Significant stress concentrations are observed near the paddle attachments and the shaft's midsection,

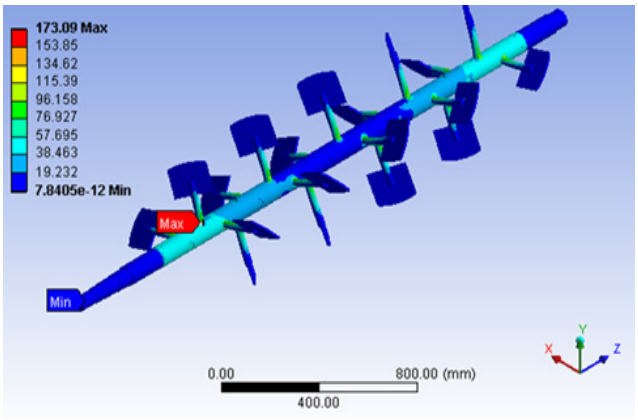


Figure 14. Maximum stresses in paddle shaft case 2.

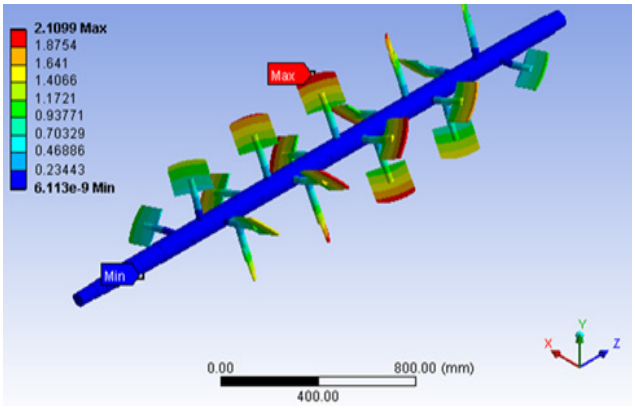


Figure 15. Maximum deformation for case 2.

indicating potential failure points where material strength is crucial. Figure 15 depicts the total deformation of the original paddle mixer shaft under loading. The maximum displacement of 2.1099 mm occurs near the middle and paddle regions, whereas the shaft ends remain nearly stationary, confirming that they are fixed or constrained. The color shading highlights greater displacement along the paddle edges, where applied forces are most impactful.

A comparative analysis was conducted on two paddle shaft configurations—one with stiffeners and one without—under identical pressure loading conditions:

- The stiffened shaft (100,000 nodes) exhibited a maximum deformation of 1.5 mm and maximum stress of 105.26 MPa.
- The unstiffened shaft (178,541 nodes) experienced higher deformation (2.1 mm) and maximum stress (173.05 MPa).

Considering the allowable stress limit of 125 MPa for structural steel, the stiffened shaft (Case 1) meets the design criteria and is selected as the optimal configuration.

4.0 Experimental Validation

A hydrostatic test was conducted on the paddle shaft to assess maximum deformation under a fluid pressure of 7.7×10^{-2} MPa, with the motor and gearbox operating at a peak temperature of 50°C. An HBM strain gauge, positioned at the center of the paddle plate, was used to measure deformation. The test was carried out at a fluid pressure of 7.7×10^{-2} MPa, and the results were compared with Finite Element (FE) Analysis predictions. The FE Analysis estimated a maximum deformation of 1.544 mm, while the experimental measurement recorded 1.82 mm, resulting in a percentage error of 8.0% between the analytical and experimental findings.

Key performance observations:

- Current Draw: The system consumed 15.1-15.3A, lower than the required 21A.
- Noise Level: Slightly exceeded the limit (95 dB vs. 90 dB).
- Vibration: Measured at 2.1 mm/sec/0, within acceptable limits.
- Temperature: Remained within the safe range (39-42°C vs. 50°C max).
- RPM: Slightly above the target (39 vs. 38).

A load trial was also performed with the tank filled to 75% capacity with water, and all measured parameters were found to be within acceptable limits, with only minor deviations in noise and RPM. Overall, the system operated close to expectations.

5.0 Result and Conclusion

Two paddle shaft designs were analyzed to identify the optimal configuration for meeting the mixer's operational requirements, which include withstanding 0.77 MPa pressure, operating at 38 rpm, and completing a load trial. ANSYS software was used for stress analysis, employing hexagonal and tetrahedral meshing. The key findings are as follows:

- Stress Analysis: The stiffened paddle shaft (Case 1) exhibited a maximum stress of 105.26 MPa, whereas the unstiffened shaft (Case 2) experienced 173.5 MPa.
- Deflection: The stiffened shaft showed a maximum deflection of 1.5 mm, while the unstiffened shaft deflected 2.1 mm.
- Deflection Location: The highest deflection was observed at the outer edge of the paddle plate.
- Stress Concentration: The maximum stress occurred at the junction where the paddle plate shaft connects to the main pipe.
- Experimental Validation: A comparison between analytical and experimental results revealed a percentage error of 8.0%, confirming the accuracy of the analysis.

6.0 References

1. Bibire L, Chitimus AD, Ciubotariu V. Design of mixing device shafts based on a proposed calculation method supported by finite element method analysis. Machines. 2024; 12(7):479. https://doi.org/10.3390/machines12070479
2. Jin XL, Jing L, Ma BJ. Kneading mixer paddles parameterized modeling. Advanced Materials Research. 2013; 655:257-263. https://doi.org/10.4028/www.scientific.net/AMR.655-657.257
3. Fan Z, Sun W. Finite element analysis of mixer shafts critical speed of differential velocity stirring kneader. Journal of Qingdao University of Science and Technology. 2008; 29:1.
4. Munteanu MG, De Bona F, Bressan F. Shaft design: A semi-analytical finite element approach. Mechanics-Based Design of Structures and Machines. 2018; 46(2):184-195. https://doi.org/10.1080/15397734.2017.1322976
5. Abbaszadeh A, Ghobadian B, Najafi G, Motevali A. Analytical and FEM design of mixing system in STR biodiesel production. Advances in Environmental Biology. 2014; 8(1):325-334.
6. Lin CM, Chang YW. Optimization designation of static mixer geometry considering mixing effect. Microsystem Technologies. 202; 27:883-892. https://doi.org/10.1007/s00542-020-04962-y
7. Kim ES, Kim BM. The shape optimal design of shaft serration using design of experiment and finite element method. Journal of the Korean Society for Precision Engineering. 2008; 25(8):72-9.
8. Xia D, Mao Z, Zhou S, He X, Wang Y. Optimized design of solid-liquid dual-impeller mixing systems for enhanced efficiency. ACS omega. 2023; 8(50):47635-47645. https://doi.org/10.1021/acsomega.3c05762

9. Jadidi B, Ebrahimi M, Ein-Mozaffari F, Lohi A. Effect of the mixer design parameters on the performance of a twin paddle blender: A DEM study. Processes. 2023; 11(3):733. https://doi.org/10.3390/pr11030733
10. Krupica A, Jirout T. Paddle mixer for viscoplastic materials and pastes. Chemical and Biochemical Engineering Quarterly. 2024; 38(2):145-152. https://doi.org/10.15255/CABEQ.2024.2289
11. Kurhade A, Talele V, Rao TV, Chandak A, Mathew VK. Computational study of PCM cooling for electronic circuit of smart-phone. Materials Today: Proceedings. 2021; 47:3171-3176. https://doi.org/10.1016/j.matpr.2021.06.284
12. Kurhade AS, Siraskar GD, Deshmukh MT, Patil PA, Chaudhari SS, Kadam AA, Dolas AS, Mahajan RG, Waware SY, Yadav RS. Impact of PCM on heat dissipation from IC Chips. J Mines Met Fuels. 2025; 73(3):717-24. https://doi.org/10.18311/jmmf/2025/47522
13. Kurhade AS, Murali G. Thermal control of IC chips using phase change material: A CFD investigation. International Journal of Modern Physics C. 2022; 33(12):2250159. https://doi.org/10.1142/S0129183122501595
14. Kurhade AS, Murali G, Rao TV. CFD approach for thermal management to enhance the reliability of IC chips.
15. Waware SY, Kore SS, Kurhade AS, Patil SP. Innovative heat transfer enhancement in tubular heat exchanger: an experimental investigation with minijet impingement. Journal of Advanced Research in Fluid Mechanics and Thermal Sciences. 2024; 116(2):51-8. https://doi.org/10.37934/arfmts.116.2.5158
16. Kurhade AS, Biradar R, Yadav RS, Patil P, Kardekar NB, Waware SY, Munde KH, Nimbalkar AG, Murali G. Predictive placement of IC chips using ANN-GA approach for efficient thermal cooling. J Adv Res Fluid Mech Therm Sc. 2024; 118(2):137-4. https://doi.org/10.37934/arfmts.118.2.137147
17. Waware SY, Chougule SM, Yadav RS, Biradar R, Patil P, Munde KH, Kardekar NB, Nimbalkar AG, Kurhade AS, Murali G, Kore SS. A comprehensive evaluation of recent studies investigating nanofluids utilization in heat exchangers. J Adv Res Fluid Mech Therm Sci. 2024; 119(2):160-72. https://doi.org/10.37934/arfmts.119.2.160172
18. Upadhe SN, Mhamane SC, Kurhade AS, Bapat PV, Dhavale DB, Kore LJ. Water saving and hygienic faucet for public places in developing countries. InTechno-Societal 2018: Proceedings of the 2nd International Conference on Advanced Technologies for Societal Applications. Springer International Publishing; 2020. p. 617-624 https://doi.org/10.1007/978-3-030-16848-3_56
19. Sidhappa KA, Hande MS, Patil MS, Mask MV. Heat transfer enhancement by using twisted tape inserts with circular holes in forced convection. International Journal of Innovations in Engineering Research and Technology. 2016; 3(3):1-7.
20. Kurhade AS, Kardekar NB, Bhambare PS, Waware SY, Yadav RS, Pawar P, Kirpekar S. A comprehensive review of electronic cooling technologies in harsh field environments: Obstacles, progress, and prospects. J Mines Met Fuels. 2024; 72(6):557-79 [Internet]. https://doi.org/10.18311/jmmf/2024/45212
21. Kurhade AS, Waware SY, Bhambare PS, Biradar R, Yadav RS, Patil VN. A comprehensive study on *Calophyllum inophyllum* biodiesel and dimethyl carbonate blends: Performance optimization and emission control in diesel engines. J Mines Met Fuels. 2024; 72(5):499-507. https://doi.org/10.18311/jmmf/2024/45188
22. Kurhade AS, Waware SY, Munde KH, Biradar R, Yadav RS, Patil P, Patil VN, Dalvi SA. Performance of solar collector using recycled aluminium cans for drying. J Mines Met Fuels. 2024; 72 (5):455-61. https://doi.org/10.18311/jmmf/2024/44643
23. Kurhade AS, Siraskar GD, Bhambare PS, Dixit SM, Waware SY. Numerical investigation on the influence of substrate board thermal conductivity on electronic component temperature regulation. J Adv Res Numer Heat Trans. 2024; 23(1):28-37. https://doi.org/10.37934/arnht.23.1.2837
24. Kurhade AS, Siraskar GD, Kondhalkar GE, Darade MM, Yadav RS, Biradar R, Waware SY, Charwad GA. Optimizing aerofoil design: A comprehensive analysis of aerodynamic efficiency through CFD simulations and wind tunnel experiments. J Mines Met Fuels. 2024: 713-24. https://doi.org/10.18311/jmmf/2024/45361
25. Kurhade AS, Siraskar GD, Darade MM, Dhumal JR, Kardile CS, Biradar R, Patil SP, Waware SY. Predicting heat transfer enhancement with twisted tape inserts using fuzzy logic techniques in heat exchangers. J Mines Met Fuels. 2024: 743-50. https://doi.org/10.18311/jmmf/2024/45348
26. Kurhade AS, Kadam AA, Biradar R, Bhambare PS, Gadekar T, Patil P, Yadav RS, Waware SY. Experimental investigation of heat transfer from symmetric and asymmetric IC Chips mounted on the SMPS board with and without PCM. J Adv Res Fluid Mech Therm Sc. 2024; 121(1):137-4. https://doi.org/10.37934/arfmts.121.1.137147

27. Patil P, Kardekar N, Yadav R, Kurhade A, Kamble D. Nanofluids: An experimental Study for MQL Grinding. J Mines Met Fuels. 2023; 71(12):2751-2756. https://doi.org/10.18311/jmmf/2023/41766
28. Patil P, Kardekar N, Yadav R, Kurhade A, Kamble D. Al_2O_3 nanofluids: An experimental study for MQL grinding. J Mines Met Fuels. 2023; 2751-2756. https://doi.org/10.18311/jmmf/2023/41766
29. Kurhade AS, Bhambare PS, Desai VP, Murali G, Yadav RS, Patil P, Gadekar T, Biradar R, Kirpekar S, Charwad GA, Waware SY. Investigating the effect of heat transfer influenced by the application of wavy corrugated twisted tape inserts in double pipe heat exchangers. J Adv Res Fluid Mech Therm Sc. 2024; 122(2):146-155. https://doi.org/10.37934/arfmts.122.2.146155
30. Kurhade AS, Murali G, Jadhav PA, Bhambare PS, Waware SY, Gadekar T, Yadav RS, Biradar R, Patil P. Performance analysis of corrugated twisted tape inserts for heat transfer augmentation. J Adv Res Fluid Mech Therm Sci. 2024; 121(2):192-200. https://doi.org/10.37934/arfmts.121.2.192200
31. Kurhade MA, Dange MM, Nalawade DB. Effect of wavy (corrugated) twisted tape inserts on heat transfer in a double pipe heat exchanger. International Journal of Innovations in Engineering Research and Technology. 2015; 2(1):1-8.
32. Kurhade AS, Gadekar T, Siraskar GD, Jawalkar SS, Biradar R, Kadam AA, Yadav RS, Dalvi SA, Waware SY, Mali CN. Thermal performance analysis of electronic components on different substrate materials. J Mines Met Fuels. 2024; 72(10):1093-1098. https://doi.org/10.18311/jmmf/2024/45569
33. Kurhade AS, Siraskar GD, Jawalkar SS, Gadekar T, Bhambare PS, Biradar R, Yadav RS, Waware SY, Mali CN. The impact of circular holes in twisted tape inserts on forced convection heat transfer. J Mines Met Fuels. 2024; 72(9):1005-1012. https://doi.org/10.18311/jmmf/2024/45505
34. Kurhade AS, Darade MM, Siraskar GD, Biradar R, Mahajan RG, Kardile CS, Waware SY, Yadav RS. State-of-the-art cooling solutions for electronic devices operating in harsh conditions. J Mines Met Fuels. 2024; 72(9):843-861. https://doi.org/10.18311/jmmf/2024/45374
35. Kurhade AS, Warke P, Maniyar K, Bhambare PS, Waware SY, Deshpande S, Harsur S, Ingle M, Kolhe P, Patil PA, Jadhav P. The wind rose analysis of temperature variation with sensor implantation technique for a wind turbine. J Adv Res Fluid Mech Therm Sci. 2024; 122(1):1-8. https://doi.org/10.37934/arfmts.122.1.118
36. Kurhade AS, Siraskar GD, Bhambare PS, Keloth D, Kaithari SM, Waware SY. Enhancing smartphone circuit cooling: a computational study of PCM integration. J Adv Res Numer Heat Trans. 2024; 27(1):132-45. https://doi.org/10.37934/arnht.27.1.132145
37. Yadav RS, Gadekar T, Gundage V, Patil P, Patil A, Patil P, Patil A, Sutar R, Kurhade AS. Numerical and experimental investigation of the effect of overlapping angle on strength and deformation of curved plate joined using arc welding process. J Mines Met Fuels. 2024; 72(10):1059-66. https://doi.org/10.18311/jmmf/2024/45697
38. Yadav RS, Nimbalkar A, Gadekar T, Patil P, Patil VN, Gholap AB, Kurhade AS, Dhumal JR, Waware SY. Comparison of experimental and numerical investigation of mono-composite and metal leaf spring. J Mines Met Fuels. 2024; 72(9):815-27. https://doi.org/10.18311/jmmf/2024/45325
39. Deshpande SV, Pawar RS, Keche AJ, Kurhade A. Real time surface finish measurement of stepped holding shaft by automatic system. Journal of Advanced Manufacturing Systems. 2025. https://doi.org/10.1142/S0219686725500386
40. Kurhade AS, Siraskar GD, Bhambare PS, Murali G, Deshpande SV, Warke PS, Waware SY. Simulation and analysis of heat transfer in counter-flow helical double-pipe heat exchangers using CFD. International Journal of Modern Physics C. 2025. https://doi.org/10.1142/S0129183125500433
41. Parkar A, Yadav RS, Chopade R, Dhavase N, Dhumal JR, Mankar SP, Patil S, Ghuge K, Giri B, Kurhade AS. Automating the two-dimensional design of Heating, Ventilation, Air Conditioning, and Refrigeration (HVACR) ducts using computer programming language: an algorithmic approach. J Mines Met Fuels. 2025; 73(1):211-20. https://doi.org/10.18311/jmmf/2025/47335
42. Kurhade AS, Siraskar GD, Darade MM, Murali G, Katkar TR, Patil SP, Charwad GA, Waware SY, Yadav RS. Enhancement in heat transfer with nanofluids in double-pipe heat exchangers. J Mines Met Fuels. 2025; 73(1):165-172. https://doi.org/10.18311/jmmf/2025/47225
43. Kurhade AS, Chougule SM, Kharat PV, Kondhalkar GE, Murali G, Raut PN, Charwad GA, Waware SY, Yadav RS. Integrated approach to enhance vehicle safety: a novel bumper design with energy-absorbing mechanisms. J Mines Met Fuels. 2025; 73(1):27-35. https://doi.org/10.18311/jmmf/2025/47168

44. Raut PN, Dolas AS, Chougule SM, Darade MM, Murali G, Waware SY, Kurhade AS. Green adsorbents for heavy metal removal: a study on zinc ion uptake by *Tinospora cordifolia* Biocarbon. J Mines Met Fuels. 2025; 73(1):21-5. https://doi.org/10.18311/jmmf/2025/47121
45. Yadav R, Nimbalkar A, Kirpekar S, Patil PJ, Dalvi SA, Jadhav PA, Kurhade AS, Wakchaure GN. Effect of transformed-induced plasticity steel plate thickness on ultimate tensile strength of butt-welded joint using Nd: YAG Laser. International Journal of Vehicle Structures and Systems. 2024; 16(6).
46. Yadav RS, Gandhi P, Veeranjaneyulu K, Gaji R, Kirpekar S, Pawar D, Khairnar YS, Patil S, Kurhade AS, Patil SP. Influence of plate thickness on the mechanical behaviour of mild steel curved plates: an experimental study. J Mines Met Fuels. 2024; 72(12):1319-27. https://doi.org/10.18311/jmmf/2024/46253
47. Kurhade AS, Bhambare PS, Siraskar GD, Mukesh S, Dixit PS, Waware SY. Computational study on thermal management of IC chips with phase change materials. Journal of Advanced Research in Numerical Heat Transfer. 2024; 26(1):34-43
48. Kurhade MA, Dange MM, Nalawade DB. Fuzzy logic modeling of heat transfer in a double pipe heat exchanger with wavy (corrugated) twisted tape inserts. International Journal of Innovations in Engineering Research and Technology. 2015; 2(1):1-8.